

Estimation of Dynamic Stresses in Last Stage Steam Turbine Blades under Reverse Flow Conditions

J. S. Rao
Chief Science Officer
Altair Engineering
Mercury 2B Block, 5th Floor
Prestige Tech Park
Sarjapur Marathhalli Outer Ring Road
Bangalore 560 087
js.rao@altair.com

K. Ch. Peraiah
Managing Director
Arani Power Systems Ltd.
3rd Floor, Icon Block
Satyanarayana Enclave
Madinaguda
Hyderabad 500 050
peraihkch@aranipower.com

and

Udai Kumar Singh
UKS Consultants
Trendles, Ryme Intrinseca, Sherborne DT9 6JX
England
uksconsult@yahoo.com

Abstract

Last stage steam turbine blades are known to suffer high alternating stresses under low volumetric flows of steam. The low volumetric flows result in a reverse flow condition and the resulting response is unstable vibration that occurs predominantly at fundamental mode of the blade. Besides the high alternating stresses, the last stage blades are also subjected to severe centrifugal load stress that when combined with the alternating stress is responsible for fatigue failures. This paper presents a method of assessing the steady and dynamic stresses under low volumetric flows.

1.0 Introduction

Steam turbine blades are subjected to centrifugal loads from high rotational speeds apart from steam bending forces. The blades are subjected to excitation frequencies ranging from the rotational speed and its harmonics. There are other

excitations depending on the number of nozzles or vanes in each respective stage together with their harmonics. Therefore, it is inevitable that some blades or other in the flow path are subjected to resonance near the operational speed. In any case all the blades are subjected to some form of resonance during start up or shutdown operations and in some cases at speeds very close to operational speed, see Rao (1991).

In such blades that may operate in near-resonant conditions close to the operating speed, the designers have to provide sufficient damping to give the desired life, Rao and Saldanha (2003) These blades are susceptible for failures, unless very close grid frequency control is maintained as in Narora last stage blades, Rao (1998a).

In other typical off-design running operations that are commonly encountered one of the serious considerations lies in operations with much lower steam flow conditions, e.g., operation under half the throughput of steam as against designed condition. In such a case of extreme operation conditions one might see a reverse flow condition in the last stage steam turbine blades. This reverse flow is known to be a primary source of instability with the response at the fundamental natural frequency at a given rotational speed.

Under low volumetric flows, the dynamic stresses of the blading are caused by partly complicated unsteady flows. The magnitude of excitation is to be assessed under these conditions. While theoretically this may be possible with today's computational power, the best way of determining the unsteady pressure distribution is through specially designed experimental approach. Gloger et. al., (1989) described an LP model turbine in which the flow field over the complete 360° circumference before and after the end-stage blade can be measured by turning the outer diffusion wall. An end stage was investigated at this model turbine at low volumetric flow and high back pressure. It was found that the detectable turbulence with hub separation and drifting of flow to the blade tip (reverse flow) is responsible for the high alternating stress as experience by the blade due to excitation of all relevant vibration forms.

This paper describes a method of assessing steady and dynamic stresses using the pressure measurements made under low volumetric flow conditions by Singh (1999).

2.0 Blade Data

Normal operating speed of machine = 8500 RPM

Blade Material X20Cr13 / X20CrMo13

Density = 7700 kg/m³

Poisson's ratio = 0.3

Ultimate tensile strength S_u = 880 MPa (at operating temp, 50.4 C)

Yield stress S_y = 575 MPa (at operating temp, 50.4 C)

Young's Modulus E = 218000 MPa (at operating temp, 50.4 C)

Lazan's coefficient J = 30 kNm/m³/cycle

Lazan's exponent = 2.4

An unsteady fully 3D viscous analysis developed earlier by Singh (1999) was used for the evaluation of both steady and unsteady pressures over the last stage rotor blade surfaces of the turbine. The effects of the potential as well as the viscous interactions that exist between the two rows in a turbo machine stage are included. The steady state pressures (at 10 points along the chord on pressure and suction surfaces from 0 to 100% span in 10 steps) given in table 1 are the time averaged pressures derived from the unsteady pressure field due to the interaction for one rotor passing period through the stator pitch. A combined steady state analysis of all the three stages together was first conducted to lay down the boundary conditions for the inlet to the third stage. However, the inlet boundary conditions for the unsteady analysis of the third stage were corrected for the incoming wake effects arising from the second stage. The unsteady pressures at any point on the rotor blade surface vary randomly with the flow conditions. As the inlet mass flow is lowered, parts of the rotor span particularly regions near the hub experience reverse flow. The extent of this reverse flow grows as the inlet mass flow is lowered substantially from its design value. Although in reality unsteady analysis for this third stage were undertaken for much reduced mass flows and were of the order of 10% of the design mass, the results given in this paper are for a much higher mass which was of 20% order. This was mainly due to difficulties with the finite element modeling at lower mass flows. Further simplifications were also made to the variations in the unsteady peaks of negative and positive pressure fluctuations from their time averaged values. It was assumed that the peaks of negative and positive unsteadiness were of equal magnitude and also these fluctuations in pressures from their time averaged values adhered to cosine form with a phase angle shift which varied from a reference location on the leading edge of the rotor. The exact location of the reference point depended on the loci of the end point of the reverse flow at the leading edge. These assumptions were made to facilitate and ease the input data for the finite element analysis, a brief description of which is given below.

Table 1 Steady steam pressures - Pa

		Pressure Surfaces									
HUB		TIP									
x/cax	0% Span	10% Span	20% Span	30% Span	40% Span	50% Span	60% Span	70% Span	80% Span	90% Span	100% Span
0	9000	9060	9120	9180	9240	9300	9620	9940	10260	10580	10900
0.1	7900	7920	7940	7960	7980	8000	8280	8560	8840	9120	9400
0.2	8060	8168	8276	8384	8432	8600	8940	9280	9620	9960	10300
0.3	8220	8356	8432	8628	8764	8900	9200	9500	9800	10100	10400
0.4	8350	8500	8650	8800	8950	9100	9360	9620	9880	10140	10400
0.5	8400	8580	8760	8940	9120	9300	9520	9740	9960	10810	10400
0.6	8440	8606	8772	8938	9104	9270	9436	9722	9948	10174	10400
0.7	8480	8634	8788	8942	9096	9250	9480	9710	9940	10170	10400
0.8	8520	8661	8802	8943	9084	9225	9440	9655	9870	10085	10300
0.9	8560	8688	8816	8944	9072	9200	9400	9600	9800	10000	10200
1	8600	8716	8832	8948	9064	9180	9354	9528	9702	9876	10050

x/cax	Suction Surfaces											
	HUB	0%	10%	20%	30%	40%	50%	60%	70%	80%	90%	TIP
	Span	Span	Span	Span	Span	Span	Span	Span	Span	Span	Span	Span
0	9000	9060	9120	9180	9240	9300	9620	9940	10260	10580	10900	
0.1	8300	8700	9100	9500	9900	10300	10760	11220	11680	12140	12600	
0.2	8150	8380	8610	9070	9070	9300	9600	9900	10200	10500	10800	
0.3	8100	8260	8420	8580	8740	8900	9080	9260	9440	9620	9800	
0.4	8150	8280	8410	8540	8670	8800	9000	9200	9400	9600	9800	
0.5	8200	8320	8440	8560	8680	8800	9000	9200	9400	9600	9800	
0.6	8290	8392	8494	8596	8698	8800	9000	9200	9400	9600	9800	
0.7	8370	8456	8542	8628	8714	8800	9000	9200	9400	9600	9800	
0.8	8460	8552	8644	8736	8828	8920	9096	9272	9448	9624	9800	
0.9	8530	8634	8738	8842	8946	9050	9225	9400	9575	9750	9925	
1	8600	8716	8832	8948	9064	9180	9354	9528	9702	9876	10050	

3.0 Finite element model details

The blade geometric model is shown in Fig. 1 and Fig. 2 is the FE model.

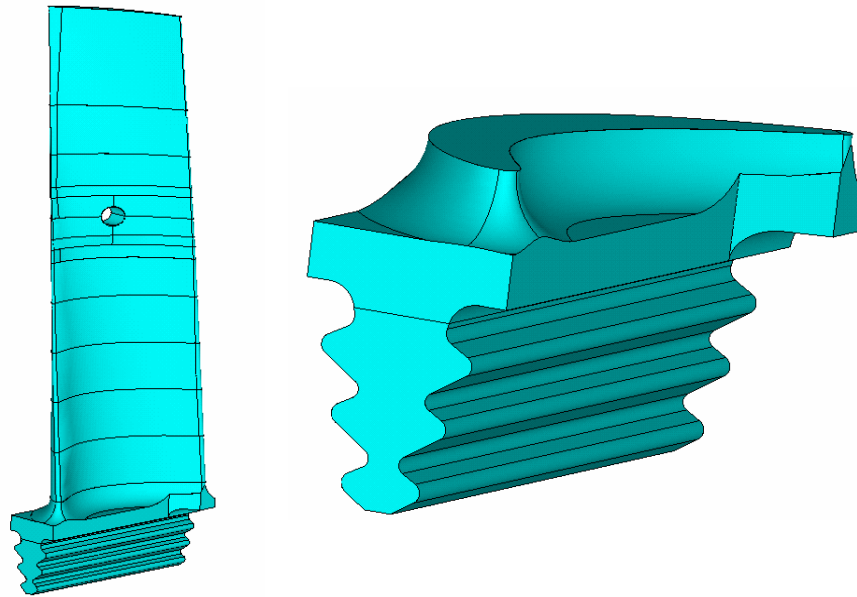


Fig. 1 Blade Geometric Model

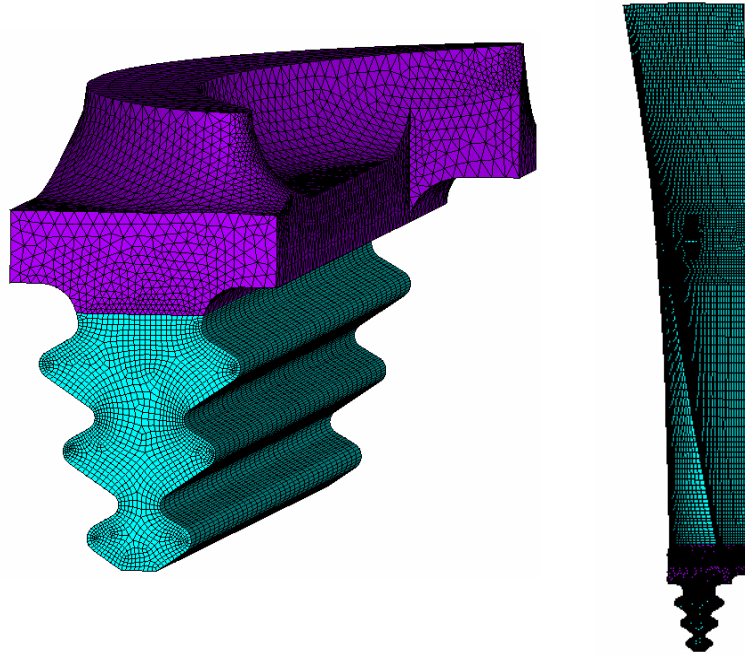


Fig. 2 F E Model of the Blade

4.0 Stress Analysis

Static stress analysis was carried out for 8500 rpm with the static steam pressure loads given in Table 1. The boundary conditions are given in Fig. 3.

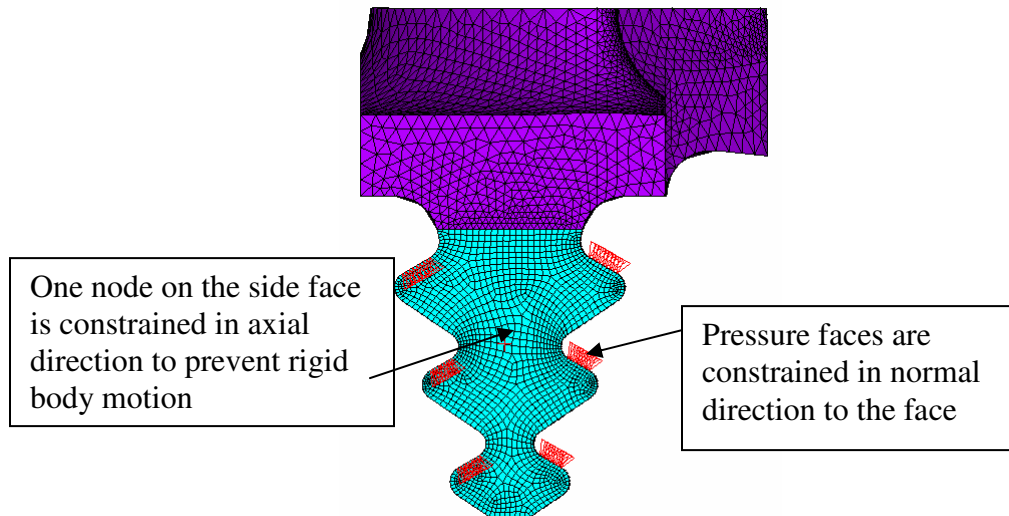


Fig. 3 Boundary Conditions

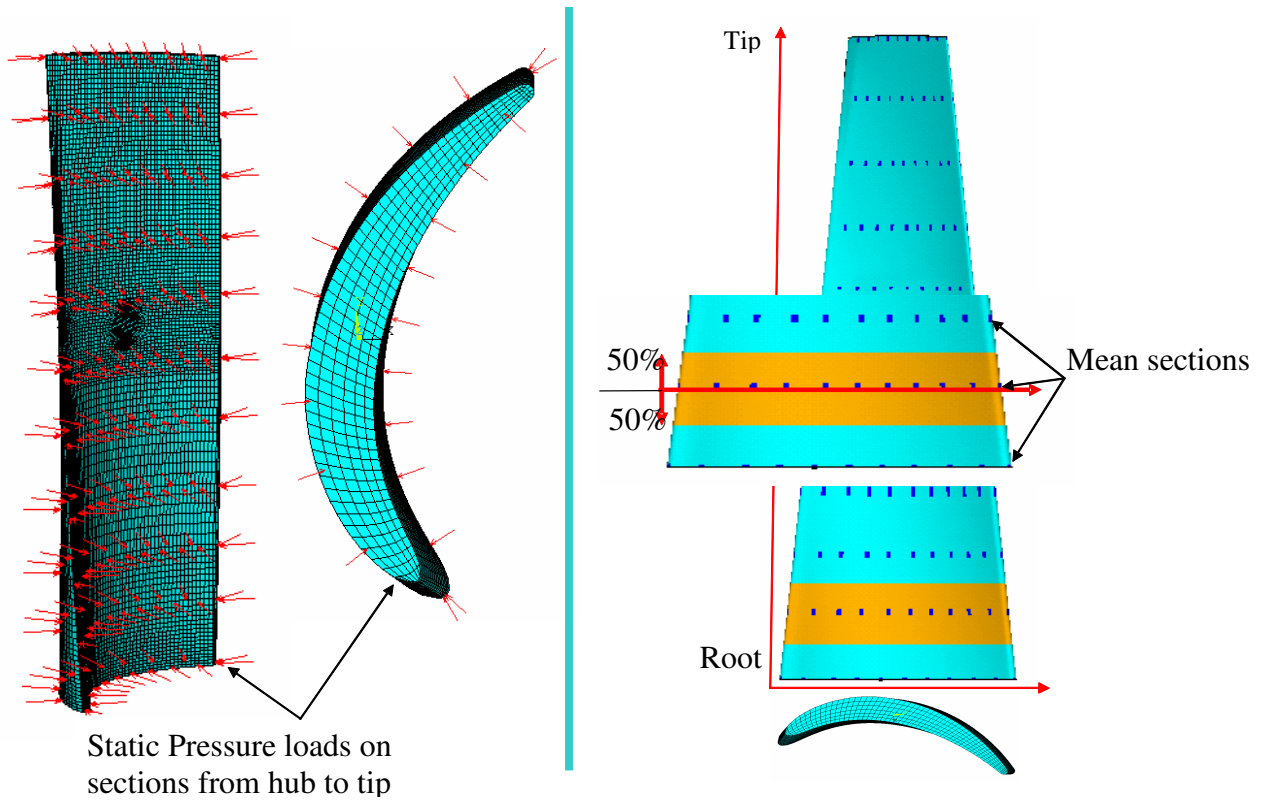


Fig. 4 Mapping of Steam Pressure loads

Steam Pressure Loads are mapped as illustrated in Fig. 4. Pressure loads applied on sections from hub to tip. Half of the elements above and below each of these sections receive the same pressure.

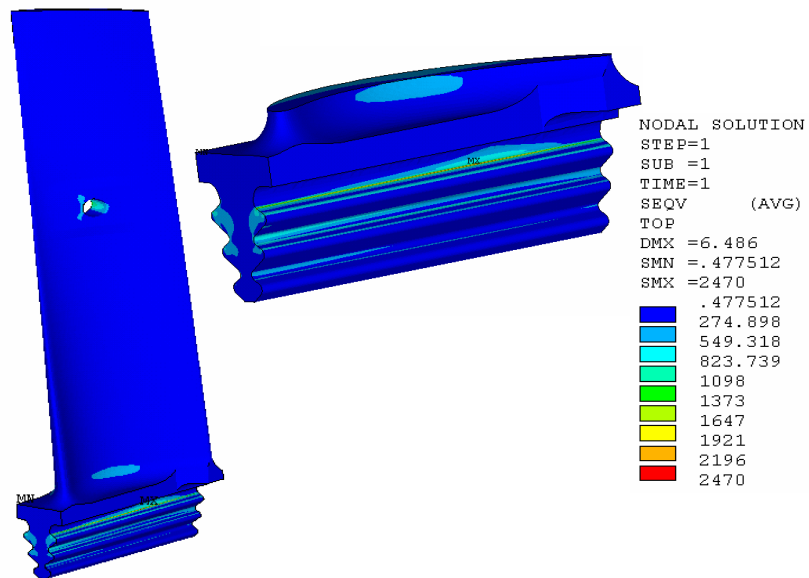


Fig. 5 von Mises Stress plot due to Centrifugal Load

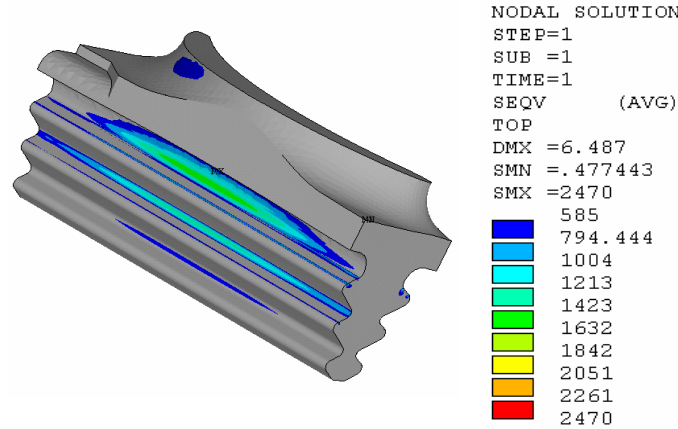


Fig. 6 Plastic region beyond yield 585 MPa of Fig. 5

Static Steam loads are negligible and the maximum stress observed is 4 MPa only. The centrifugal load causes maximum stress and the peak value is 2470 MPa far beyond the yield as shown in Fig. 5. The blade otherwise is globally elastic with an average stress 343 MPa. The plastic region is small in depth and elastic analysis is not applicable here, that is why we have a highly unrealistic value. The plastic region beyond yield 585 MPa is shown in Fig. 6. The depth of the max stress is 1 element and the element depth is 0.37mm.

No elasto-plastic analysis was carried out as local stress and strain are estimated to determine life by Strain based methods. An elasto plastic analysis will not change the global elastic region, the limited plastic region results will be limited to be just above yield.

A free vibration analysis is carried out and from the Campbell diagram it is found that, 344.50707 Hz 1F is the critical natural frequency for single blade in self excited vibration. The 1F mode is considered for damping estimation and life estimation.

5.0 Unsteady Loads

The unsteady pressures are defined in the form given from measurements made under unstable reverse flow conditions (which are not too dissimilar from the present case) as briefly described by Chana and Singh (2005).

$$\frac{dp}{P_{o1}} \cos(\omega t + \psi)$$

$$P_{o1} = 2000 \text{ N/m}^2$$

$$\psi = \text{Phase angle}$$

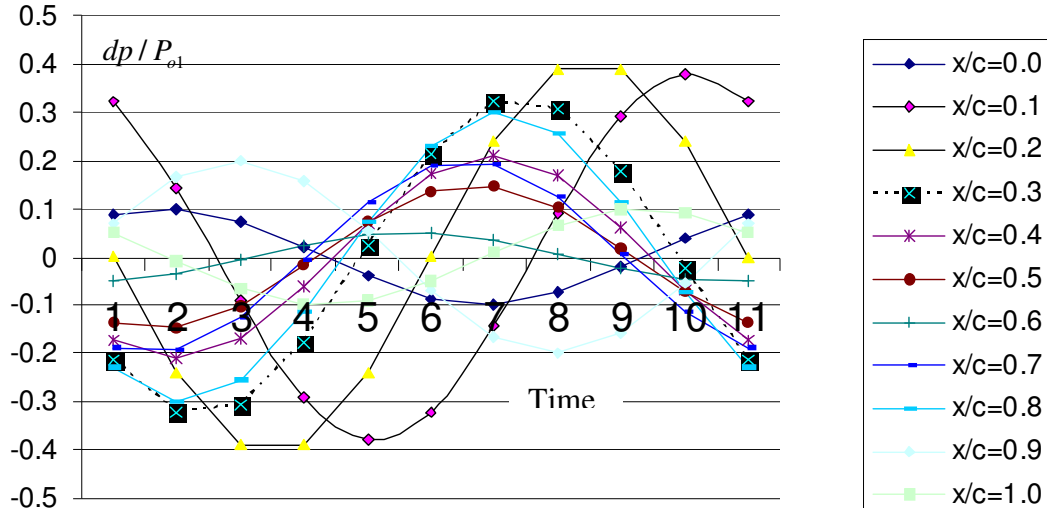


Fig.7 Unsteady Pressure

Fig. 7 gives the harmonic variation of the pressure at the hub. Similarly pressure values are prepared along the blade span at 10% intervals and across the aerofoil section at 10 points from leading edge to trailing edge.

6.0 Harmonic Analysis

Alternating pressure is applied in the form

$$\frac{dp}{P_{o1}} \cos(\omega t + \psi) 2000 \times 10^{-6}$$

where, $P_{o1} = 2000 \text{ N/m}^2$

Table 2 gives the real and imaginary parts of the pressures that take into account the phase at hub as given in Fig. 7. These pressures are calculated on similar lines and given at different spans of the blade from root to tip and also from leading edge to trailing edge of aerofoil profile. These values are applied on the full span of blade by considering 50% elements above and below of mean sections of the blade span from root to tip as shown in Fig. 4.

In order to obtain the equivalent static response with appropriate phases taken into account, a harmonic analysis is performed at very low frequency close to zero i.e. is 0.01 Hz. The average section stress is 0.13373 MPa that controls the dynamic stress value for the purpose of strain based life estimation adopted in the following sections. The peak stress at the stress raiser is 0.9547MPa.

Table 2 Real and Imaginary Pressure Components at Hub corresponding to Chord locations in Fig. 7

dp / P_{o1} (max)	$dp = \frac{dp}{P_{o1}} 2000 \times 10^{-6}$	ψ	Real part	Imaginary part
			$A \cos \psi$	$A \sin \psi$
0.1	0.0002	330	0.000173	-0.000100004
0.38	0.00076	32	0.000645	0.000402737
0.41	0.00082	90	4.96E-09	0.00082
0.33	0.00066	130	-0.00042	0.000505593
0.21	0.00042	145	-0.00034	0.000240905
0.15	0.0003	155	-0.00027	0.000126788
0.05	0.0001	190	-9.8E-05	-1.73636E-05
0.2	0.0004	160	-0.00038	0.000136812
0.3	0.0006	140	-0.00046	0.000385677
0.2	0.0004	290	0.000137	-0.00037588
0.1	0.0002	60	0.0001	0.000173205

7.0 Estimation of Damping

Damping is quantified as a function of strain amplitude at a reference point in the blade, following Rao and Saldanha (2003). ANSYS is adopted to perform all the necessary calculations. First the natural frequencies and orthonormal mode shapes are obtained at the desired speed. Lazan's damping law is used to determine the specific damping energy in each element of the blade. Total damping energy and strain energy are calculated by integrating them over the entire volume. With the help of these the loss factor is obtained. From the loss factor, the equivalent viscous damping ratio is determined.

The nonlinear damping in the first mode of the blade is obtained as shown in Fig. 9 for the reference point shown in Fig. 10. This damping relation is used in determining the resonant response.

8.0 Resonant Response

The strain at the reference point from section 6 is found to be 0.702 E-06 as shown in Fig. 10. To obtain the resonant response, a damping ratio 1.55% (0.00155) is assumed which gives the quality factor equal to 32.258. Therefore the dynamic strain at the reference point under resonance is 22.645E-06. With this strain, the damping ratio from Fig.9 is 0.0012. Further iterations are performed and the results are shown in Table 3.

Therefore the correct equivalent damping ratio at resonance is 0.00226, 0.226%. Therefore the magnification factor is

$$\frac{1}{2\xi} = 221.239$$

From Section 6, the peak steady stress is 0.9547 MPa

Therefore the peak dynamic stress is $0.9547 \times 221.239 = 211.2168$ MPa

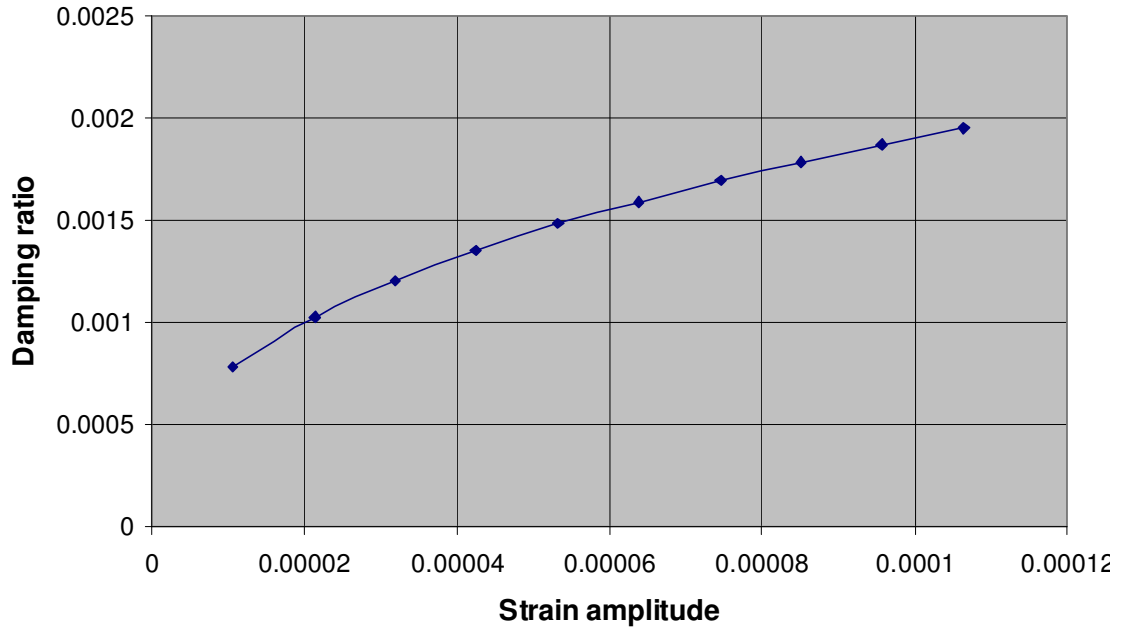


Fig. 9 Nonlinear Damping in the Blade

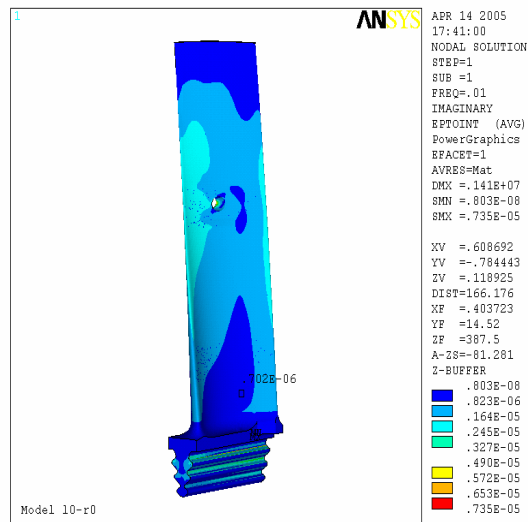


Fig. 10 Strain at Reference Point

Table 3 Iterations to determine Damping Ratio

Strain	Damping ratio	Magnification Factor	Dynamic Strain
0.702E-06	0.01550	32.2580	2.26E-05
0.702E-06	0.00120	416.667	2.93E-04
0.702E-06	0.00290	172.413	1.21E-04
0.702E-06	0.00210	238.095	1.67E-04
0.702E-06	0.00235	201.766	1.41E-04
0.702E-06	0.00225	222.220	1.56E-04
0.702E-06	0.00226	221.239	1.55E-04

9.0 Concluding Remarks

A methodology to determine dynamic stresses of last stage steam turbine blades under low volumetric flows of steam is illustrated. The alternating pressure field is estimated from test values; nonlinear material damping is estimated from Lazan's law for the fundamental mode as a function of strain amplitude at operating speed. Mean stresses are evaluated from centrifugal loads and harmonic response at the fundamental frequency is obtained from a static analysis and magnification factor obtained from an iteration process with nonlinear damping model. Dynamic stress under low volumetric flow is determined by using the magnification factor.

References

1. Chana, K. and Singh, U., (2005) Unsteady temperature and pressure measurements on the rotor surfaces of a 1.5 stage machine, DMU report TR/2290
2. Gloger, M. et. al., (1989) Design of LP Bladings for Steam Turbines, *VGB Kraftwerkstechnik*, vol. 68, No. 68, August 1989, p. 677
3. Rao, J. S., (1991) *Turbomachine Blade Vibration*, John Wiley
4. Rao, J. S., (1998a) Application of Fracture Mechanics in the Failure Analysis of A Last Stage Steam Turbine Blade, *Mechanism and Machine Theory*, vol. 33, No. 5, 1998, p. 599
5. Rao, J. S., (1998b) Crack Initiation and Propagation of Blades Fracture Mechanics Approach, Proc. Korea Fluid Machinery Association Annual Conference, February 18, 1998, p. 11
6. Rao, J. S. and Saldanha, A., (2003), Turbomachine Blade Damping, *Journal of Sound and Vibration*, vol. 262, No. 3, p. 731
7. Singh, U., (1999), Method for nucleating steam flow in low-pressure turbine stages, *Proc. of Third European Conference on Turbo Machinery IMechE publication C557/010/1999*, p.827